Cathode planarity studies in ICARUS

INTENSE Meeting 30th March 2022

Maria Artero Pons

Università degli Studi di Padova

INFN
Istituto Nazionale di Fisica Nucleare

Lar-TPC working principle - Reminder

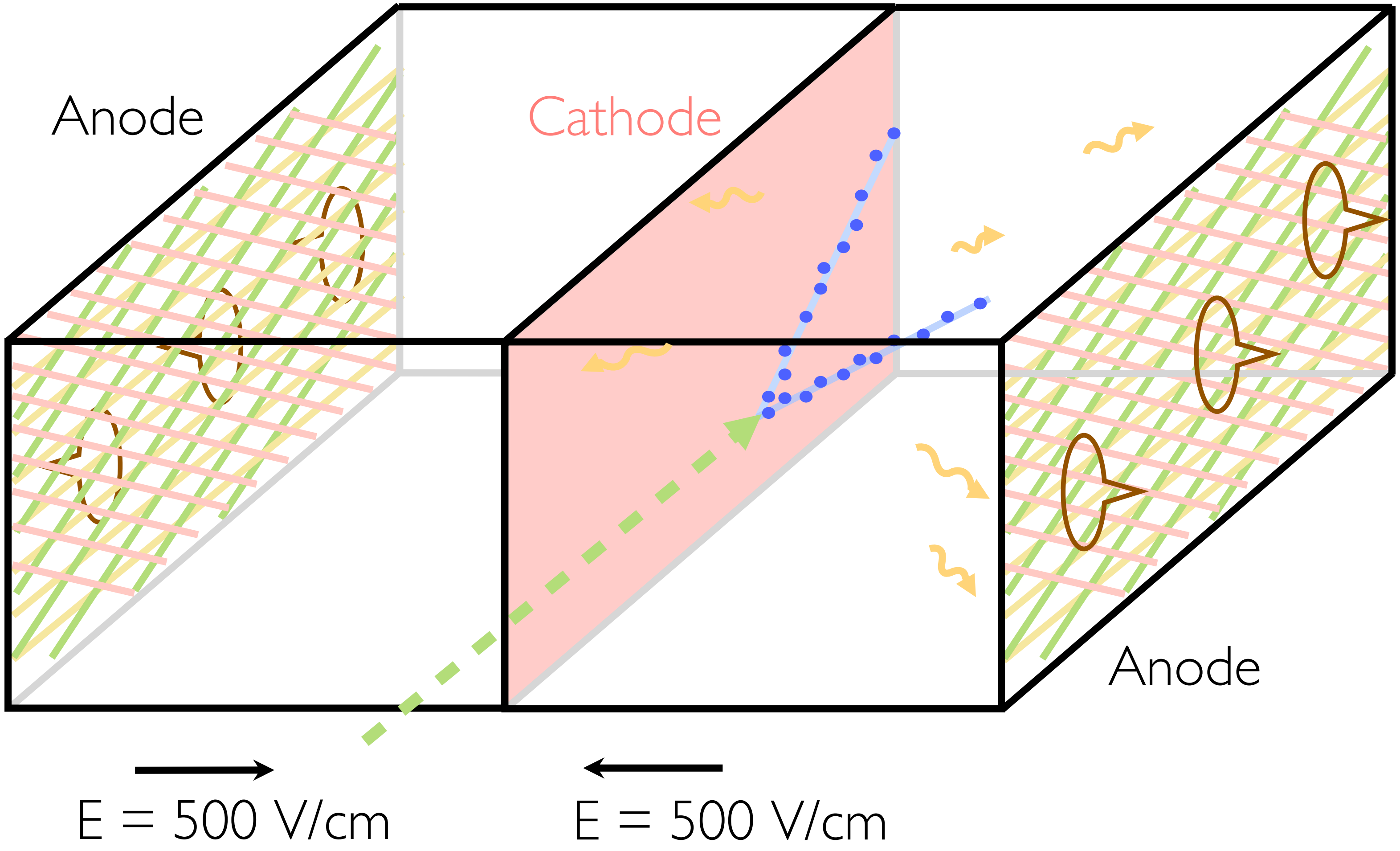

When a neutrino interacts in the Liquid Argon, it produced charged particles that deposit their energy, producing ionization electrons and scintillation light

The light propagate inside the detector and can be collected by PMTs: this signal is the basis to recognize that there has been a particle interaction in the detector

Lar-TPC working principle - Reminder

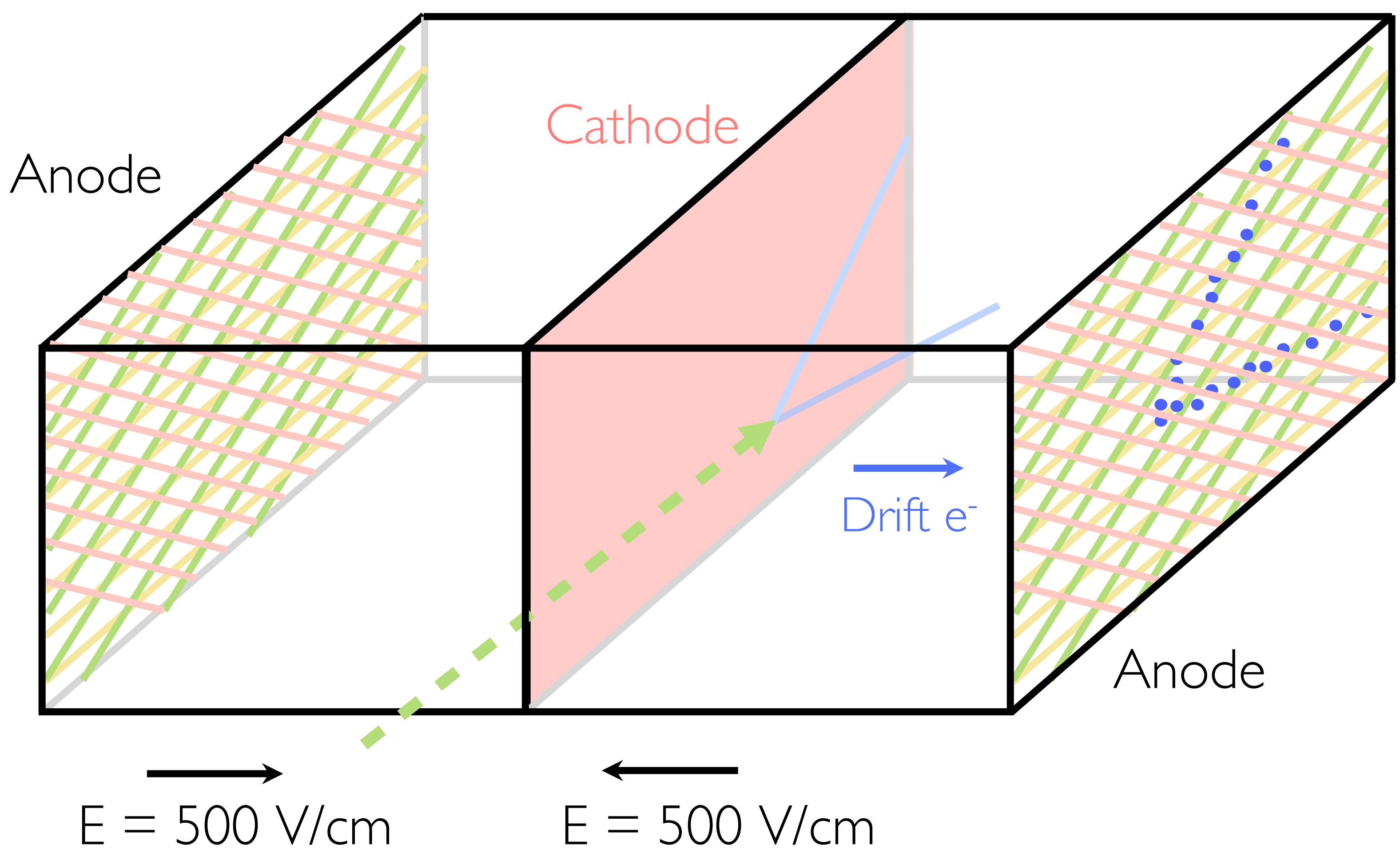

The ionization electrons produced by each ionizing particle are transported by the uniform electric field

The ionization electrons are then detected by the 3 anodic wire planes placed at the end of the drift path providing simultaneous different projections of the same event

The information from these three projections allow a precise reconstruction of the recorded particle trajectories and a precise calorimetric measurement.

Introduction

- In order to determine the absolute position of the track along the drift coordinate, we need to measure the absolute time t_0 at which the particle was crossing the detector
- Local deviations from planarity in the central cathode could affect the uniformity of the electric field causing a poorly reconstructed drift time
- In this study we test the cathode planarity by exploiting the cathode crossing cosmic muons reconstructed in the calibration ntuples
- The method relies on the difference between the maximum drift times of the tracks in the two adjacent chambers to estimate the cathode distortion at the crossing point between the TPC

Some considerations on cathode displacement

- The two TPCs on the left and right side of the cathode are symmetrical by design. Hence, in each cryostat the maximum drift distance and the electric field intensity on the L and R should be identical
    - $d_L = d_R = d_D = 148.2\ cm$
    - $E_L = E_R = E_0 = 500\ V/cm$
- For tracks crossing the cathode, the maximum drift time should also be identical on L and R chambers: $t_L = t_R = t_D$

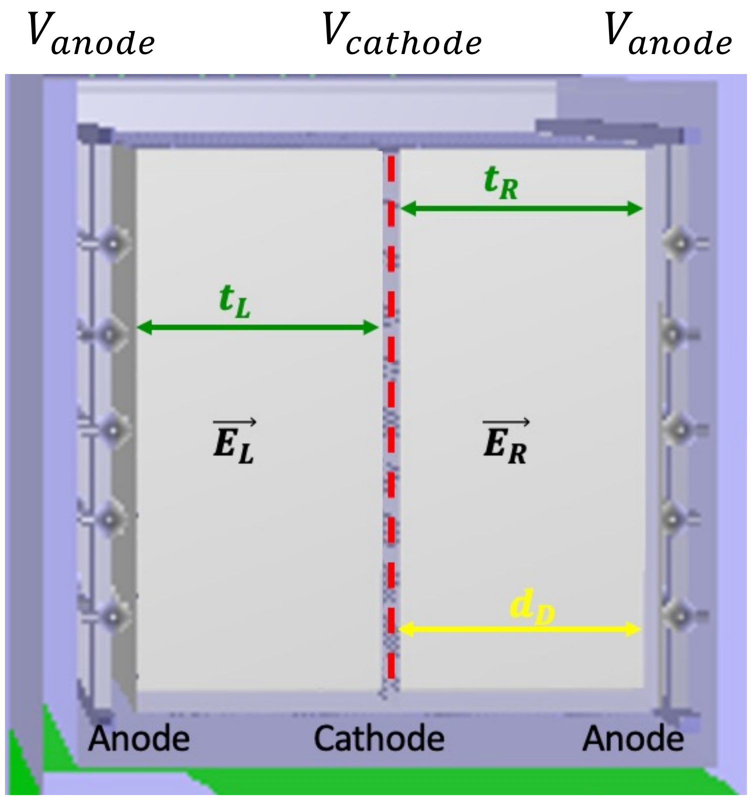

Some considerations on cathode displacement

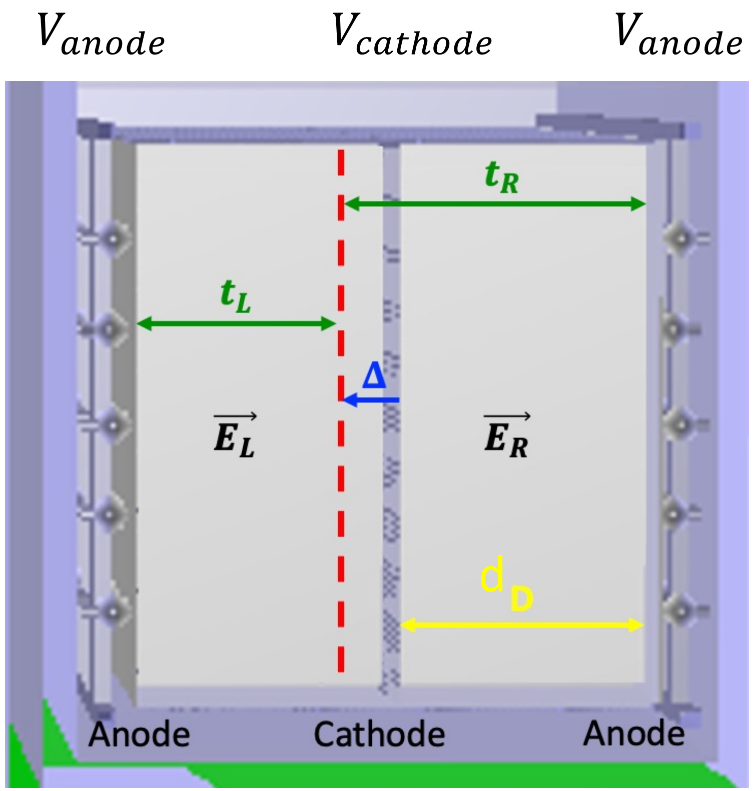

- A global displacement of the cathode $\Delta \ll d_D$ would break the L-R symmetry by changing both the drift distance and the electric field intensity,
  - $d_L = d_D - \Delta \quad d_R = d_D + \Delta \quad E_L = \frac{HV}{d_L} \approx E_0\left(1 + \frac{\Delta}{d_D}\right) \quad E_R = \frac{HV}{d_R} \approx E_0\left(1 - \frac{\Delta}{d_D}\right)$
- For small variations of the electric field around E_0, the drift velocity scales approximately like $v_{drift} \propto \sqrt{E}$

$$v_{\frac{L}{R}} = v_D \sqrt{\frac{E_{\frac{L}{R}}}{E_0}} \simeq v_D \left(1 \pm \frac{\Delta}{2 d_D}\right)$$

Some considerations on cathode displacement

- A global displacement of the cathode $\Delta \ll d_D$ would break the L-R symmetry by changing both the drift distance and the electric field intensity,
  - $d_L = d_D - \Delta \quad d_R = d_D + \Delta \quad E_L = \frac{HV}{d_L} \approx E_0\left(1 + \frac{\Delta}{d_D}\right) \quad E_R = \frac{HV}{d_R} \approx E_0\left(1 - \frac{\Delta}{d_D}\right)$
- For small variations of the electric field around E_0, the drift velocity scales approximately like $v_{drift} \propto \sqrt{E}$

$$v_{\substack{L\\R}} = v_D\sqrt{\frac{E_{\substack{L\\R}}}{E_0}} \simeq v_D\left(1 \pm \frac{\Delta}{2d_D}\right)$$

- The maximum drift time would be now

$$t_L = \frac{d_L}{v_L} = t_D\left(1 - \frac{3}{2}\frac{\Delta}{d_D}\right), \quad t_R = \frac{d_R}{v_R} = t_D\left(1 + \frac{3}{2}\frac{\Delta}{d_D}\right)$$

- The displacement Δ would correspond to

$$\Delta\,[\mathrm{mm}] = \frac{v_D}{3}\,(t_R - t_L)$$

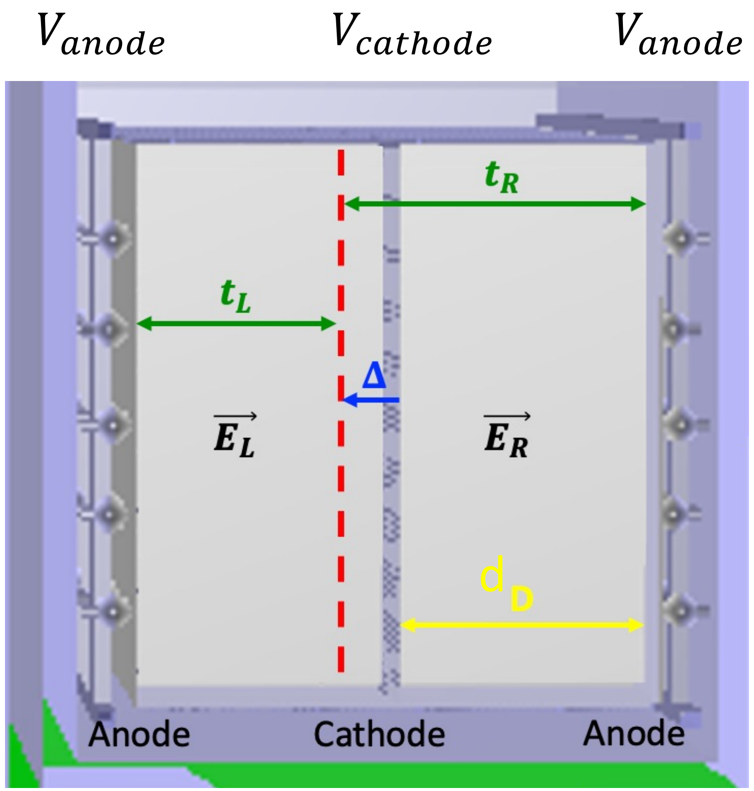

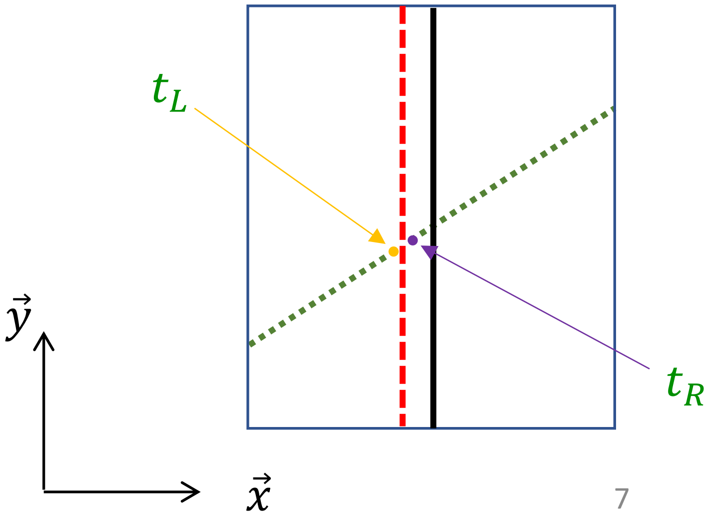

Extension of the used method

- We have derived the relation between $t_R - t_L$ and Δ considering a global displacement, but as a first approximation we can assume that the relation holds even for local cathode displacement

- The approach is the same one used during the data taking at LNGS which was tested and validated during its operation, arXiv:1612.07715

- Local cathode distortions were first measured at LAr temperature during underground operation by exploiting muons crossing the cathode, as previously described → Indirect method

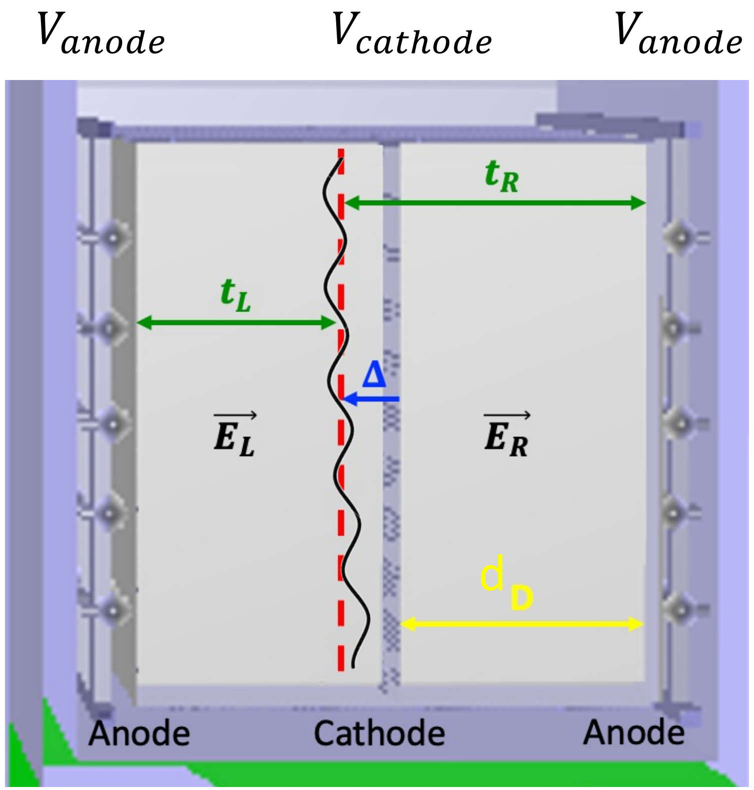

Validation of the method

- The cathode distortions were also measured during the overhaul of the detector at room temperature using a laser meter ➜ Direct method

- The two methods are independent and use information collected under very different conditions, at LAr and room temperature. So the correlation for most of the cathode panels evidenced the reliability of the methods

- A mechanical intervention after the LNGS run allowed to restore the cathode planarity within few mm

Comparison of measurement in LAr and at room temperatures

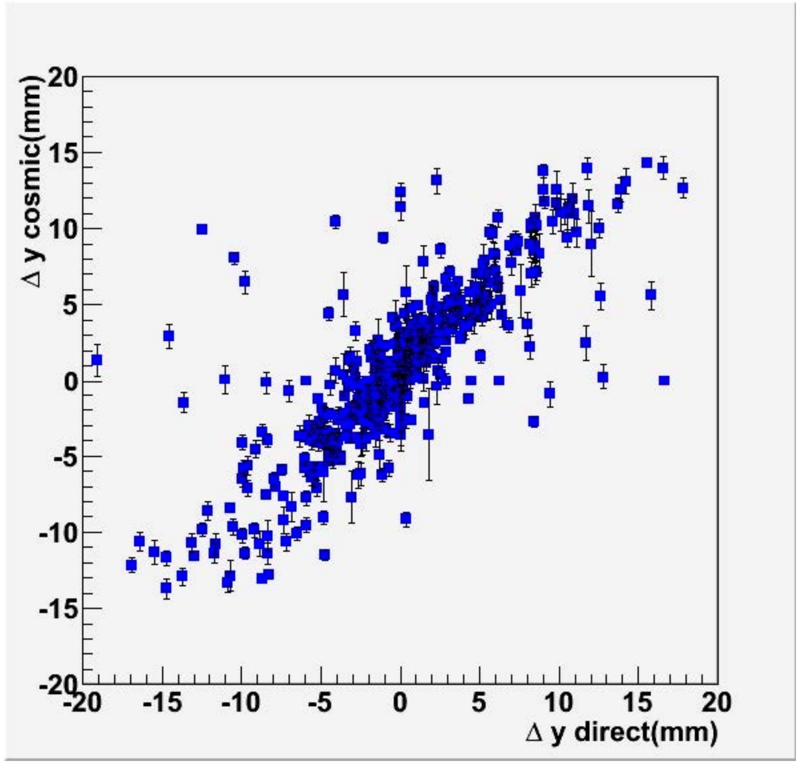

arXiv:1612.07715

Presence of Space Charge Effects (SCE)

- The difference between the underground and shallow depth performance in the detector is mainly due to the large amount of cosmic rays crossing the detector, which generate space charge effects
- Basically accumulation in the drift region of positive argon ions, which have reduced mobility causing a not negligible distortion in the drift field damaging the event reconstruction
- The electron drift velocity depends on the electric field, so any distortion will cause a delay on the electron arrival time on the anode wrt the time observed in case of uniform electric field

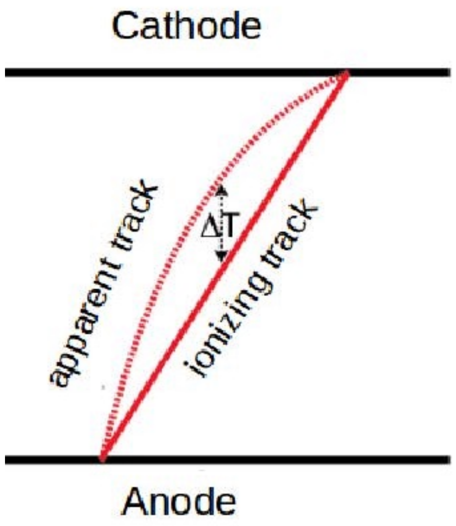

JINST 15 (2020) 07, P07001

Presence of Space Charge Effects (SCE)

- The difference between the underground and shallow depth performance in the detector is mainly due to the large amount of cosmic rays crossing the detector, which generate space charge effects
- Basically accumulation in the drift region of positive argon ions, which have reduced mobility causing a not negligible distortion in the drift field damaging the event reconstruction
- The electron drift velocity depends on the electric field, so any distortion will cause a delay on the electron arrival time on the anode wrt the time observed in case of uniform electric field

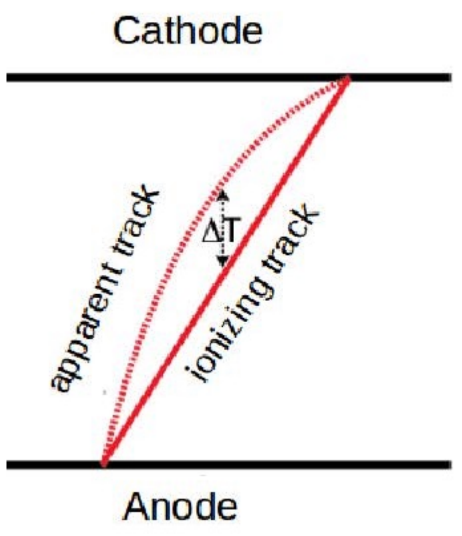

JINST 15 (2020) 07, P07001

- The time delay as a function of the drift distance was reported in JINST 15 (2020) 07, P07001, showing a small time delay because of the presence of non linear effects due to space charge
- For electrons generated at the cathode a $\approx 0.2\,\mu s$ time delay is expected from the SCE, identical in both sides of the cathode
- We can then safely neglect SCE in the following study

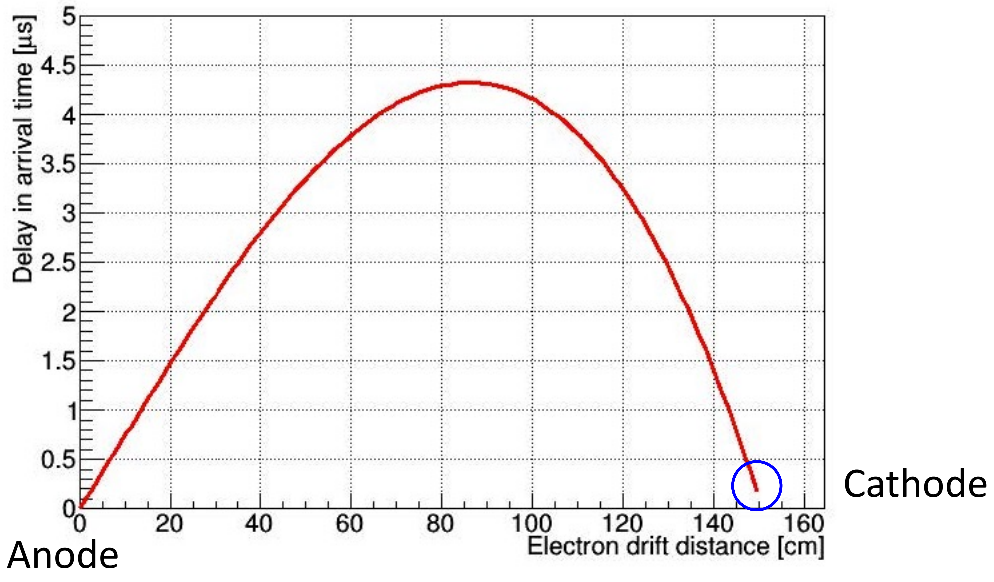

JINST 15 (2020) 07, P07001

Δ measurements

$$\Delta\,[\mathrm{mm}] = \frac{v_D}{3}\,(t_R - t_L)$$

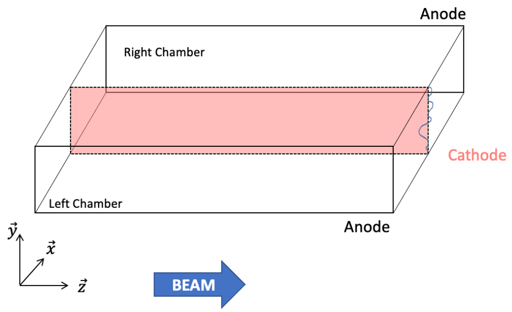

- 200k tracks were analysed, rejecting only those tagged as stopping particles

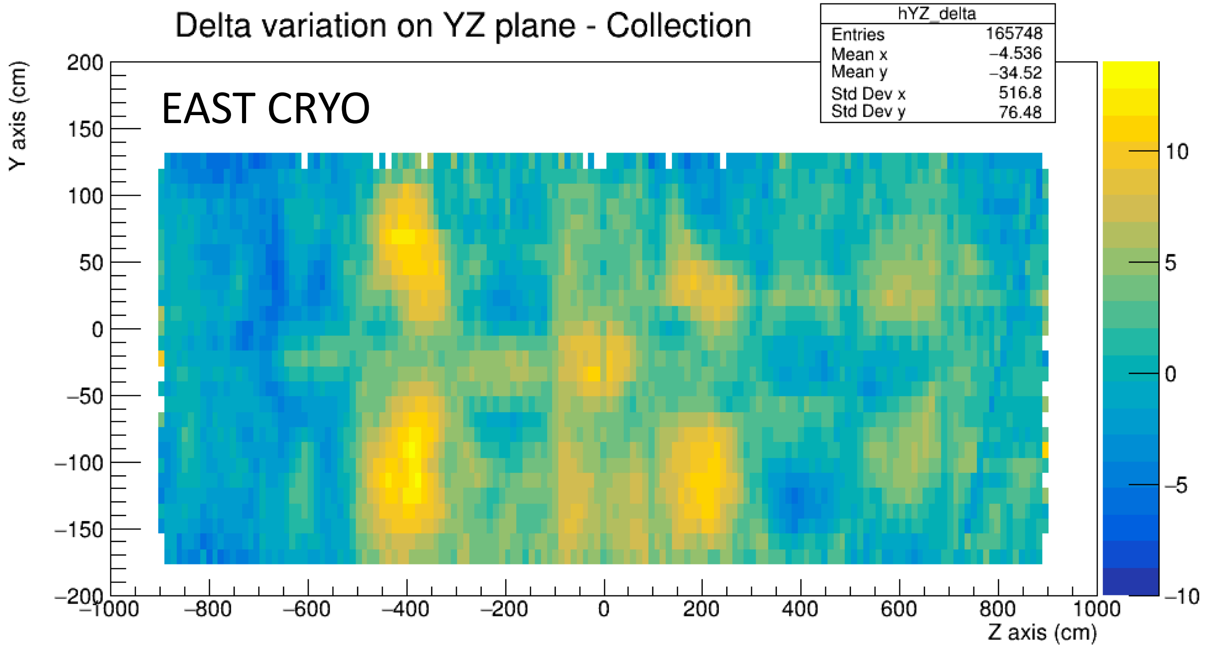

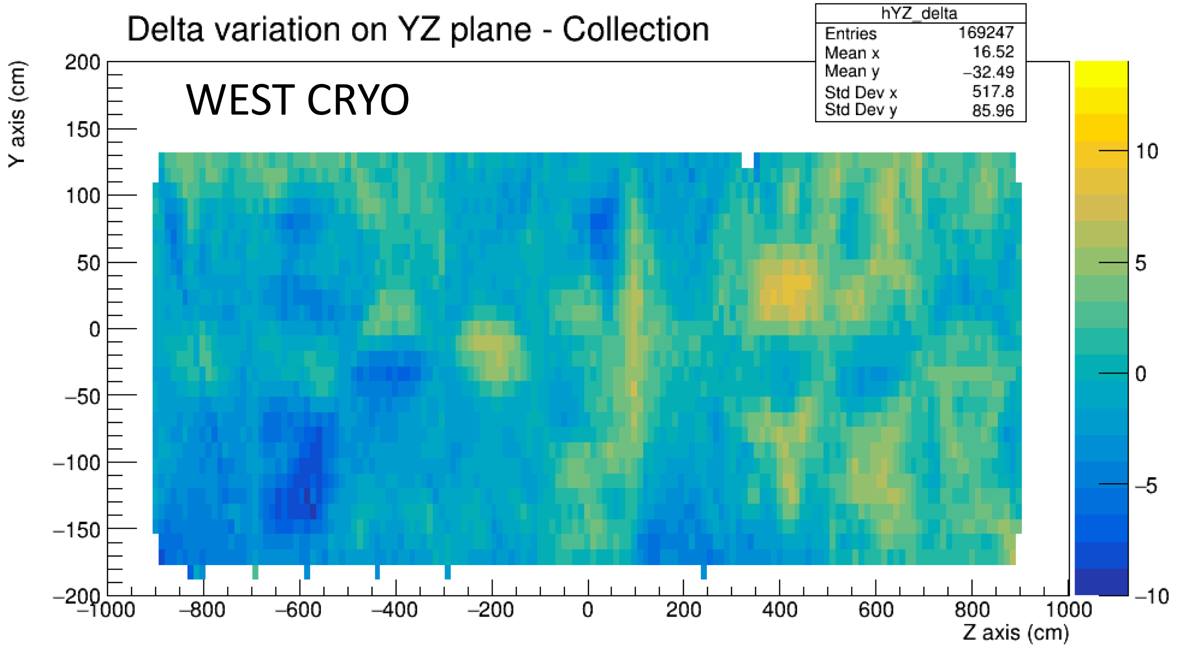

- There are local displacement in both cryostats, however the values are higher for the East module
- East variations are $(-6, 13)\ mm$, which corresponds to $\langle\Delta\rangle = 19\ mm \times \frac{1\ \mu s}{1.6\ mm} = 11.87\ \mu s$
- Instead for West the variations go from $-9\ mm$ to $9\ mm$ corresponding to $\langle\Delta\rangle = 11.25\ \mu s$

Δ measurements

- 200k tracks were analysed, rejecting only those tagged as stopping particles

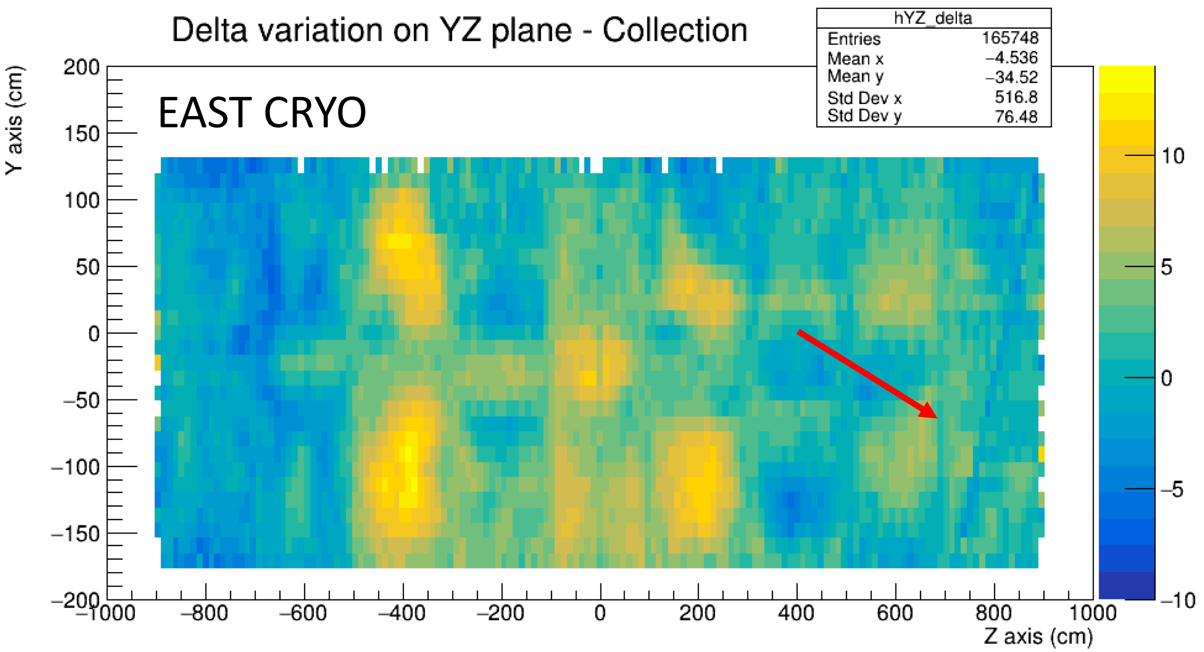

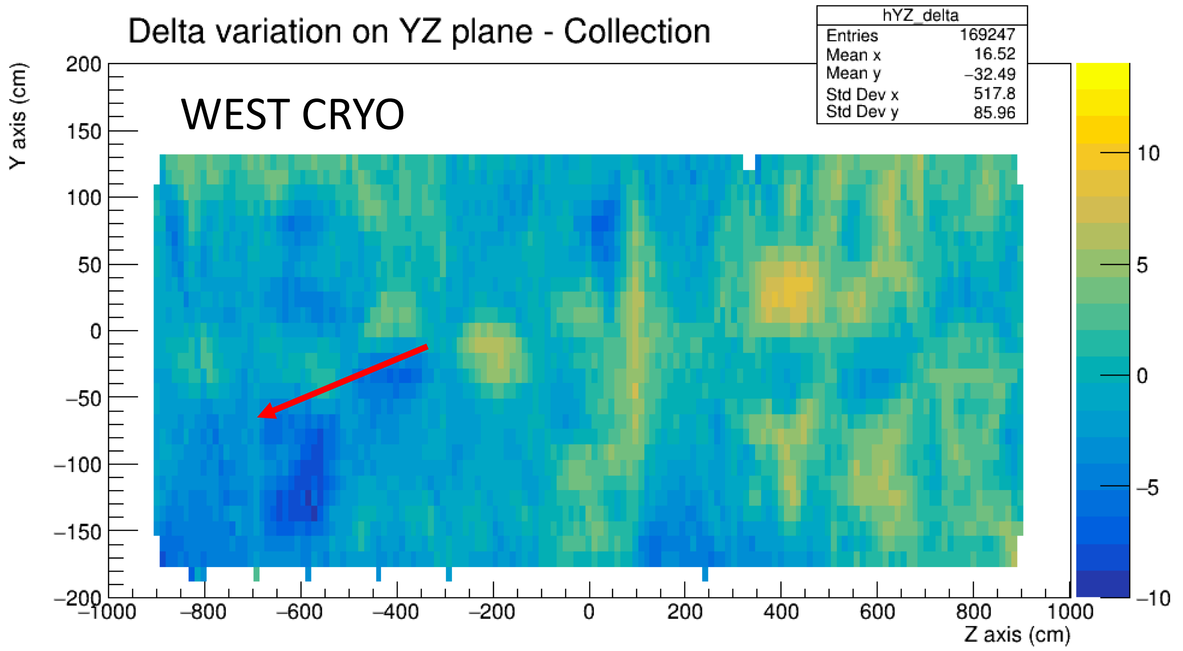

- There are local displacement in both cryostats, however the values are higher for the East module
- East variations are $(-6, 13)\ mm$, which corresponds to $\langle\Delta\rangle = 19\ mm \times \frac{1\ \mu s}{1.6\ mm} = 11.87\ \mu s$
- Instead for West the variations go from $-9\ mm$ to $9\ mm$ corresponding to $\langle\Delta\rangle = 11.25\ \mu s$
- The diagonal lines present in both TPC and with a mirrored positions with a 30° inclination, were unexpected

Cathode crossing position: Y vs Z

- In order to identify the origin of these distortions, we plot the cathode crossing points of the tracks using the two closest hits on either side of the cathode

- West cryo seems to have a more homogeneous distribution, while East cryo has a noticeable concentration in the lower part of the module

- To have a more clear vision we also plot the projections along the two axis

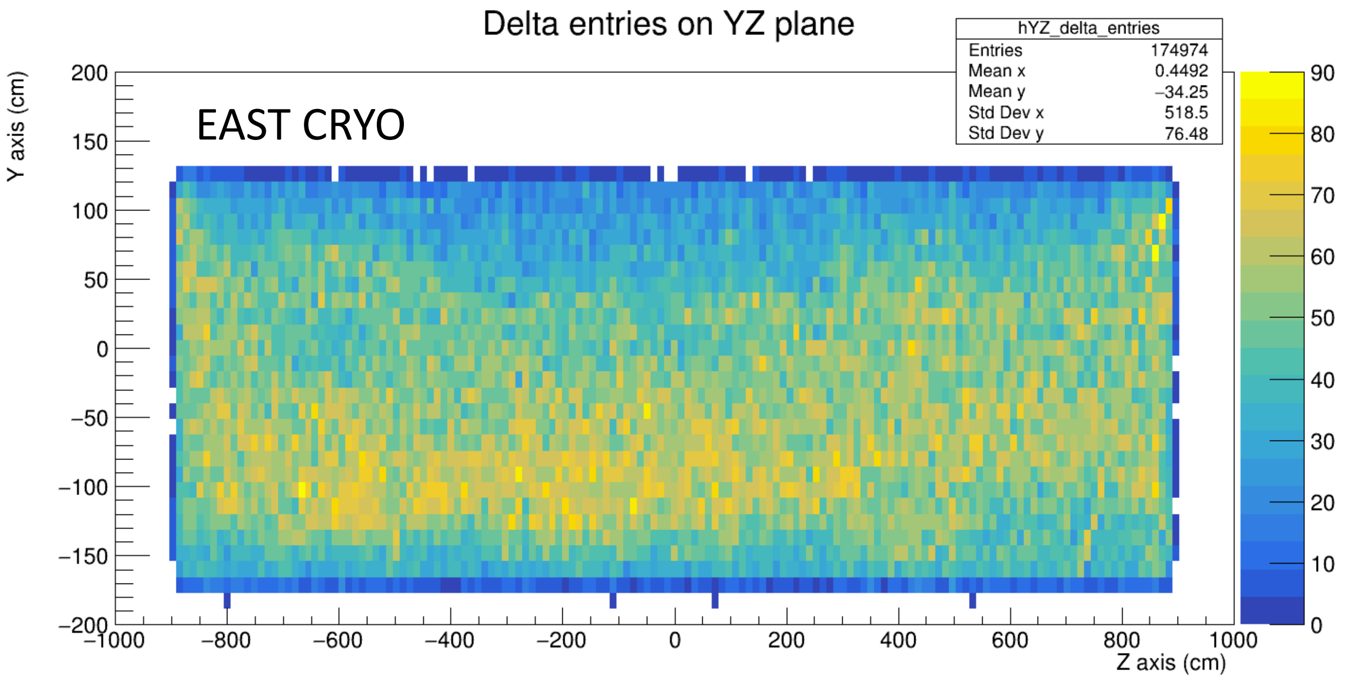

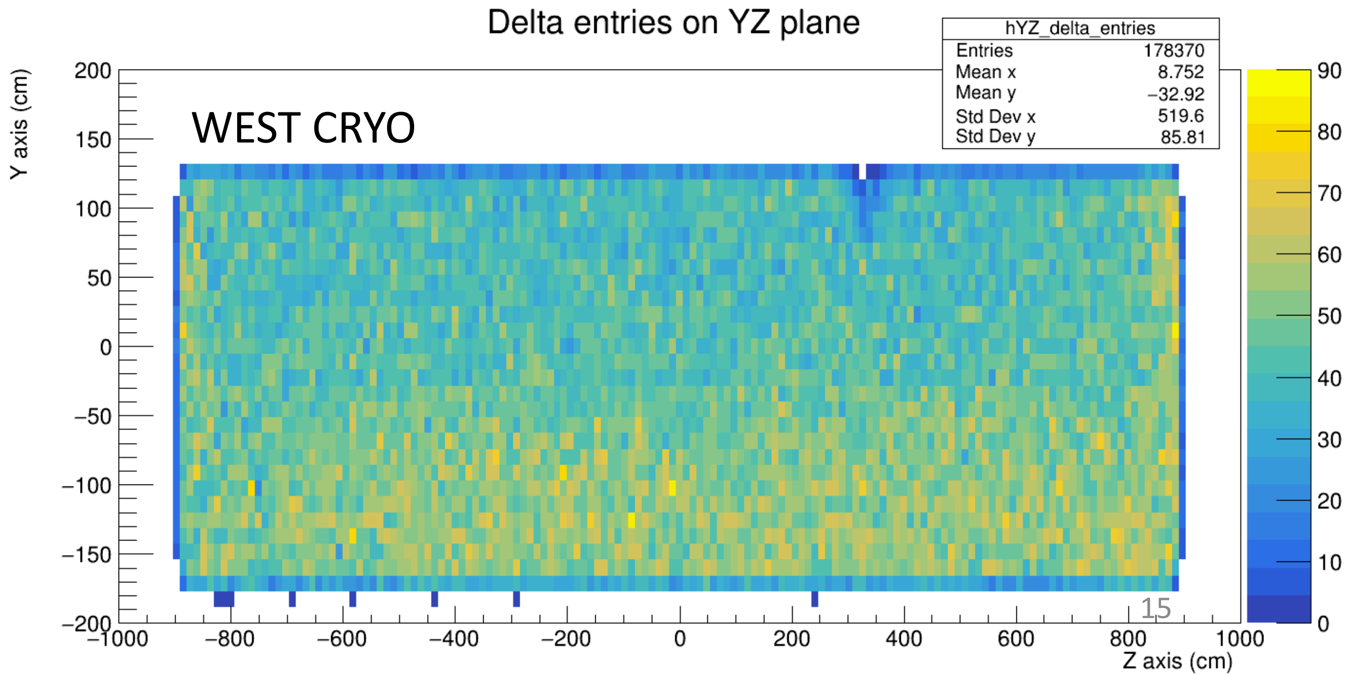

Cathode design – Technical details

Inside picture of the detector

- The cathode is composed by 9 punched panels of $3.2\,m \times 2\,m$, vertically installed with a central horizontal reinforcing bar

- Each panel has a supporting frame made by cylindrical tubes around the four borders

Cathode design – Technical details

Supporting cathode frame

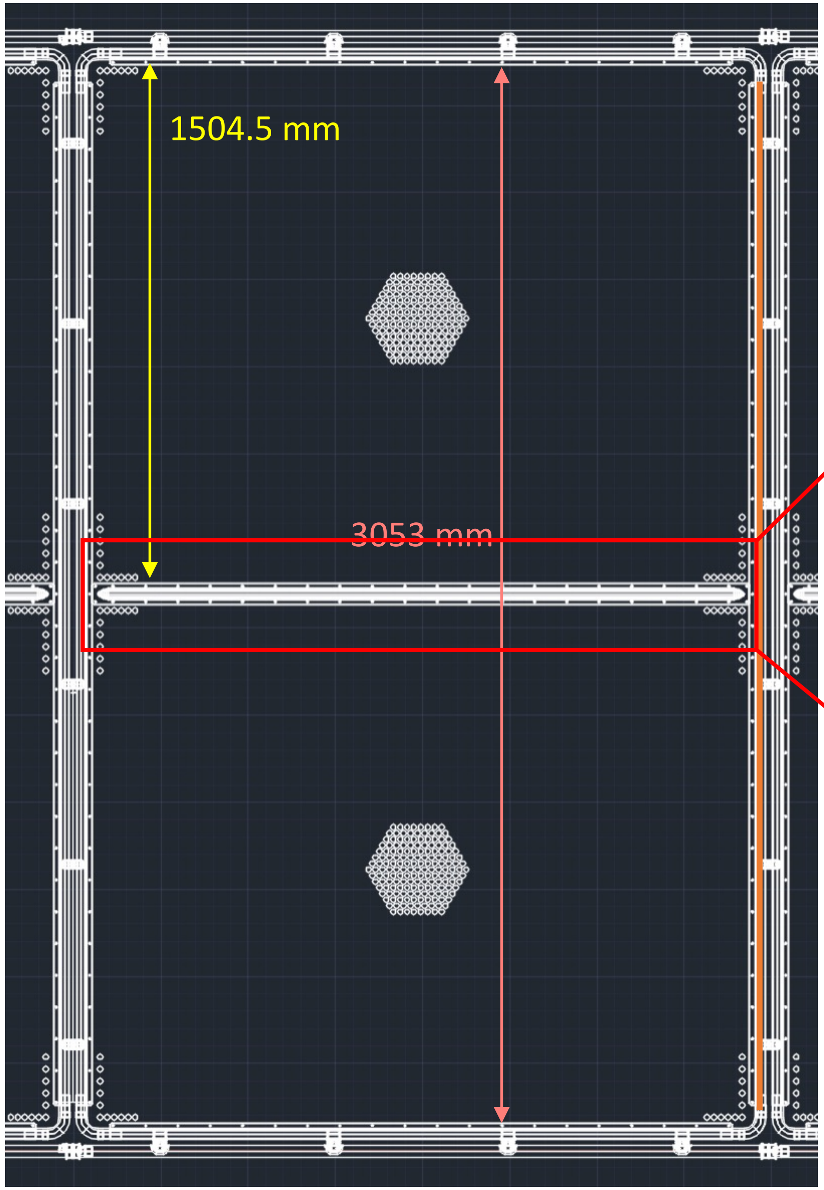

Zoom on the reinforcement bar details

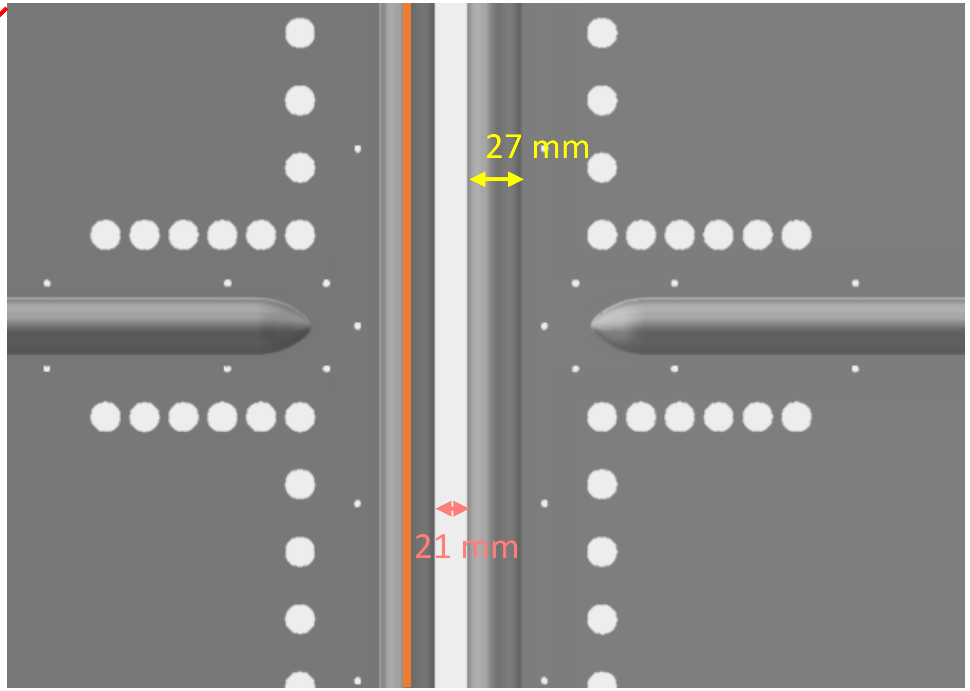

Cathode crossing position – Y projection

- The central deep is located at $y \sim -24\ cm$. We can find an explanation if we take into account the reinforcement bar placed in the middle of each cathode plane, which is preventing an efficient detection. Considering that the cathode planes are 3.2 m high and the base of the detector is at $y = -181.86\ cm$ the deep should be around $-22\ cm$

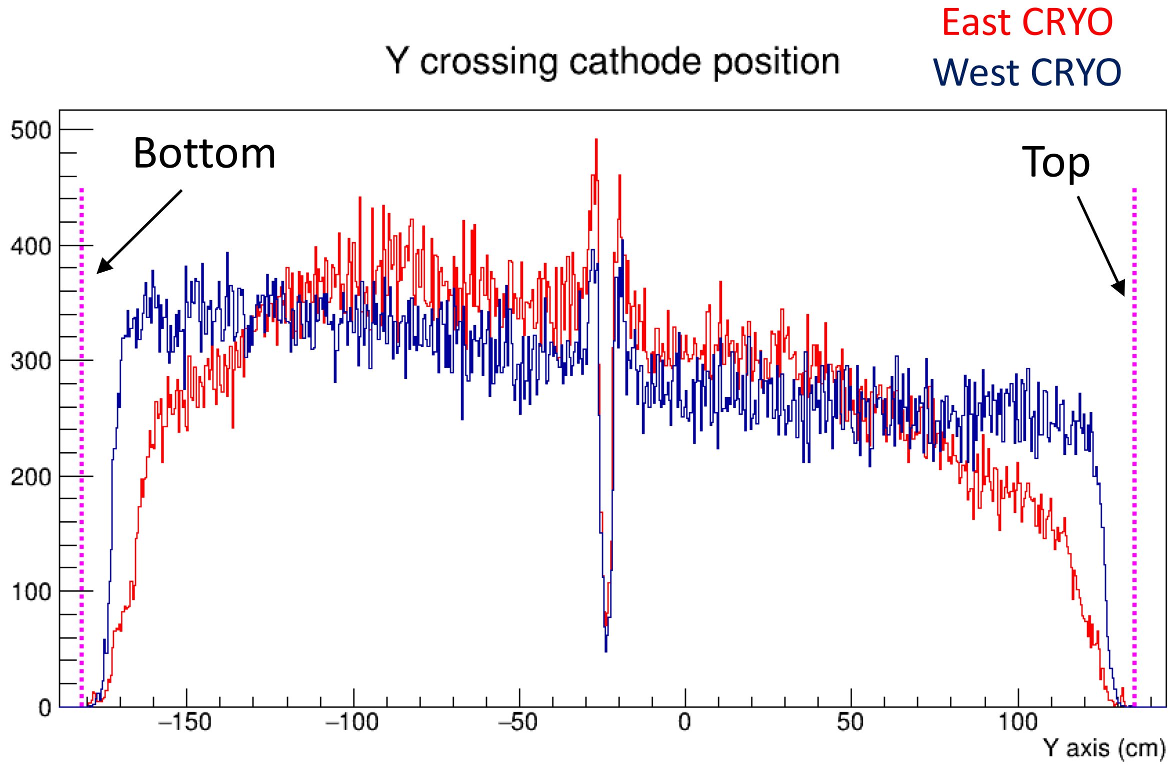

- On the sides of the valley there are a rise of events. This could be due to a distortion on the voltage by the reinforcement bar causing the tracks to curve towards the surroundings

Cathode crossing position – Y projection

- The central deep is located at $y \sim -24\ cm$. We can find an explanation if we take into account the reinforcement bar placed in the middle of each cathode plane, which is preventing an efficient detection. Considering that the cathode planes are 3.2 m high and the base of the detector is at $y = -181.86\ cm$ the deep should be around $-22\ cm$

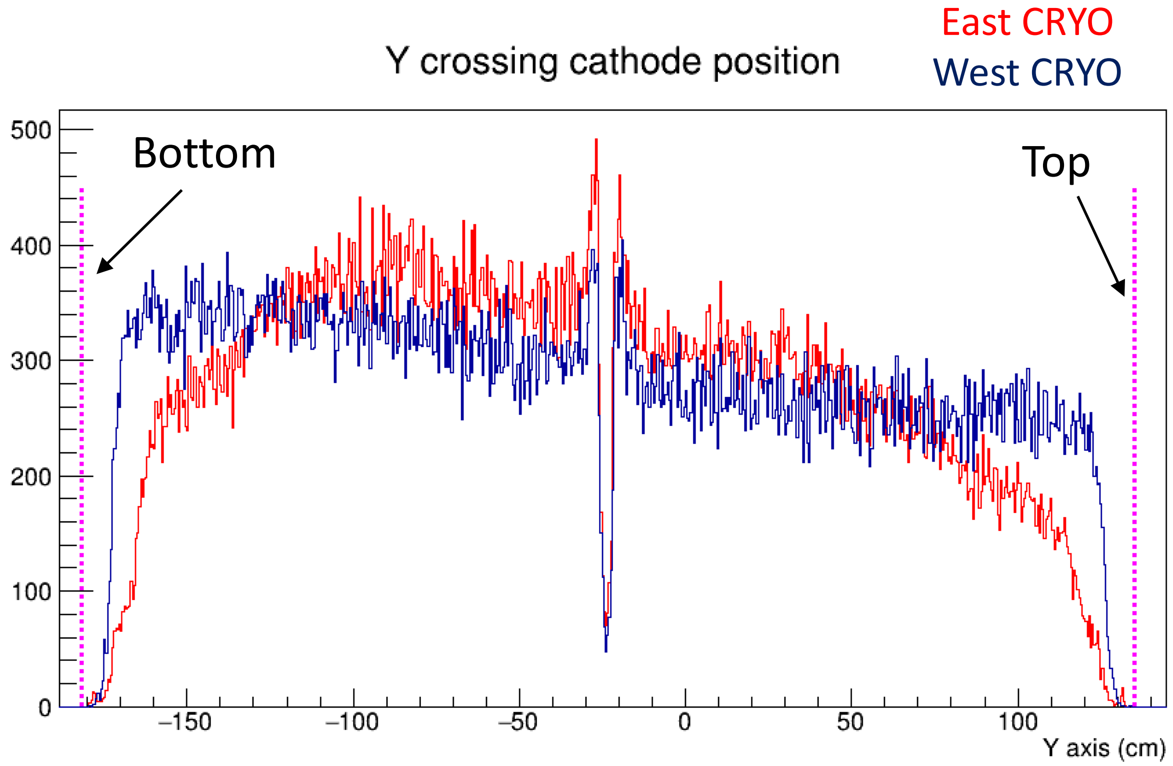

- On the sides of the valley there are a rise of events. This could be due to a distortion on the voltage by the reinforcement bar causing the tracks to curve towards the surroundings

- The distribution of entries is much more flat for the West cryo, as suggested by the previous plots. However if we take a look at the number of entries of each side of the valley we have

West Bottom	East Bottom	West Top	East Top
55.36 %	56.37 %	44.64 %	43.63 %

- The pink lines show the borders of the detector, making clear that the East cryo has problems reconstructing the hits on the top of the detector

Cathode crossing position – Z projection

- The Z distribution is much more uniform along the whole distance for both cryostats
- We can identify the 9 cathode panels, corresponding to the small deeps as this panels have tubes in their edges causing inefficiencies
- The distance between each valley is always around 2 m, in agreement with the width of the panels
- These small deeps are in reality two peak structures, which might correspond to each edge tube of the two adjacent planes. As in the Y projection each deep is surrounded by an increase of entries
- Finally, the biggest deep at $z = 0$ is not related to the cathode planes but to the wires of Induction 1, since they are split in the middle of the Z length

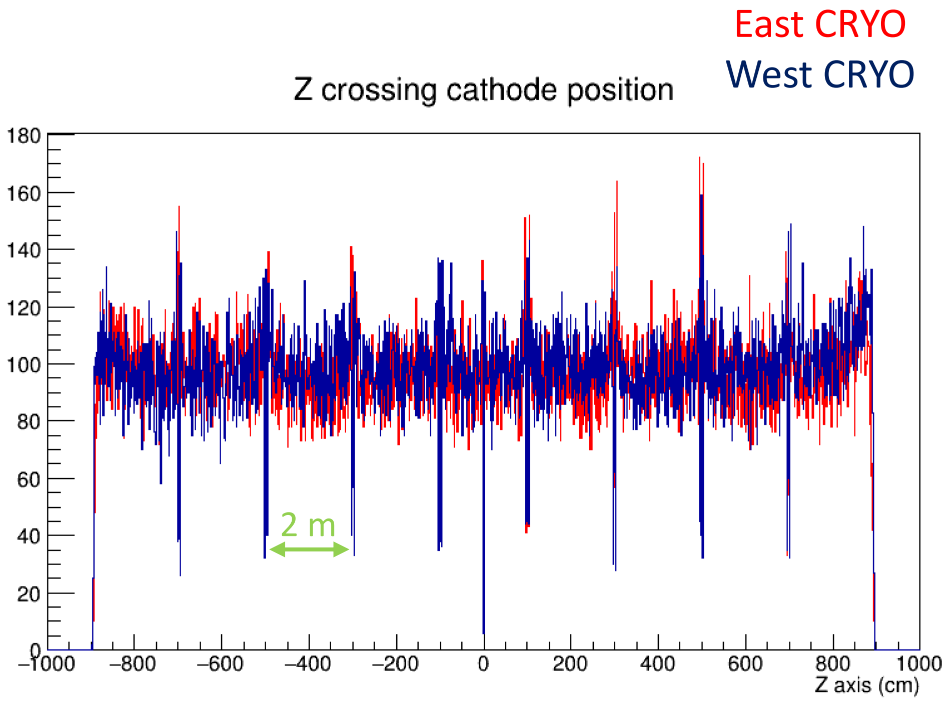

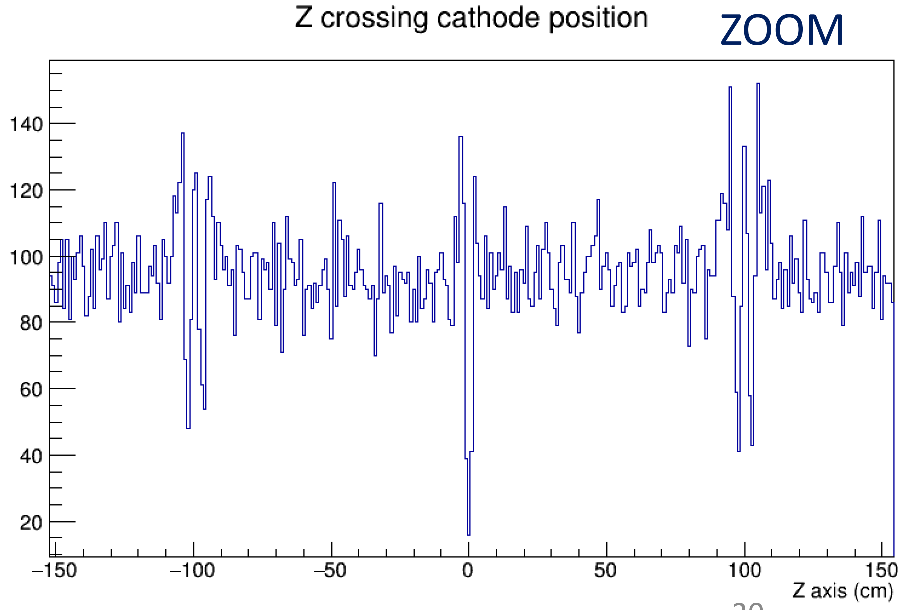

Cathode crossing position – MC comparison

- As Monte Carlo simulates a single cathode plane, there should not be any deep due to the finite dimensions of the real cathode planes, as well as the wire splitting in Induction 1
- Sample of cosmics without SCE
- MonteCarlo contains both E&W tracks together

Data MonteCarlo

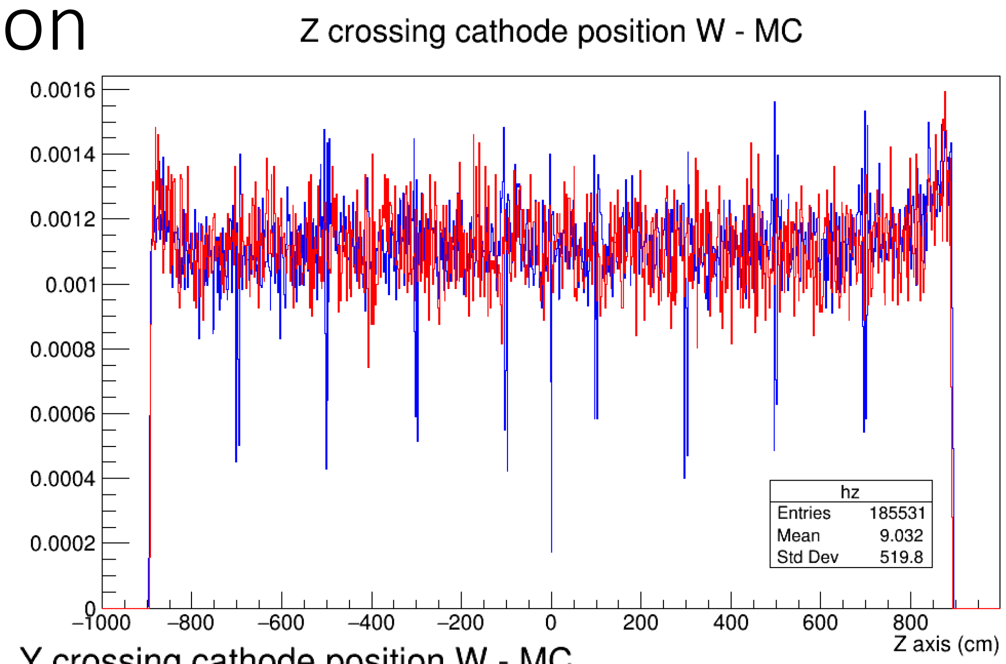

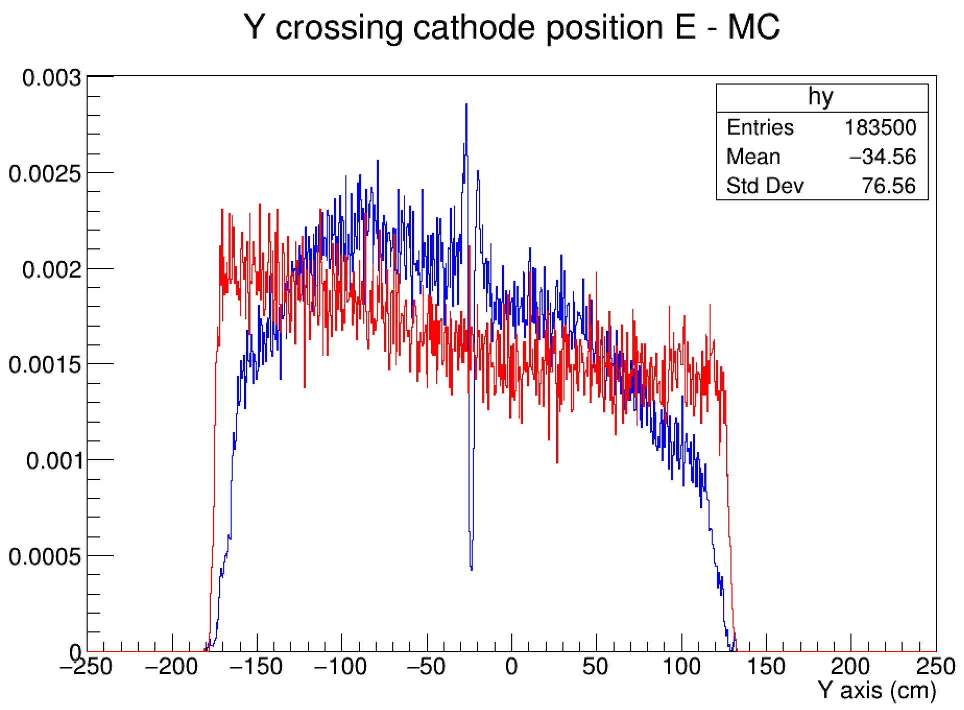

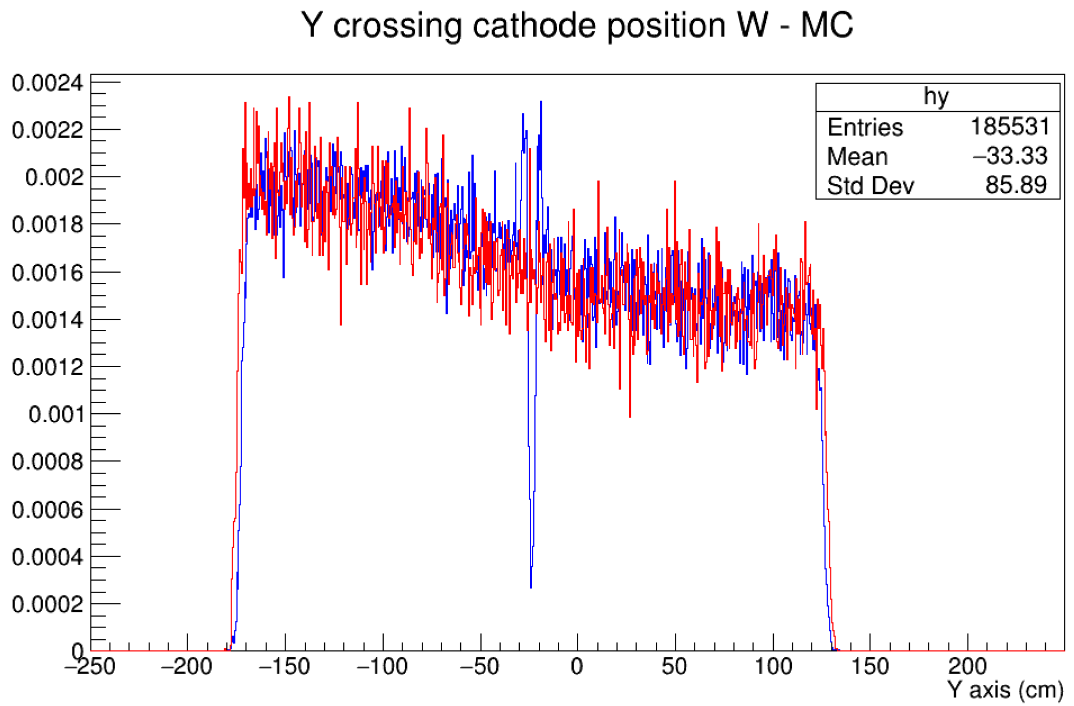

Conclusions

- We have used a validated method to estimate the cathode displacement, observing distortions in both cryostats
- There are some features which need to be better understood such as the diagonal lines or the non homogeneous distribution of entries on the different TPC
- The final plots regarding the projections shown to contain a lot of information, providing a method to spot inefficiencies during the track reconstruction
- Monte Carlo comparison proved the geometrical origin of all the deeps seen in the projections of Δ distributions

- Next steps are:

  - Compute the Δ displacement for Monte Carlo data
  - Redo the analysis using Anode to Anode tracks
  - Check everything using more data in order to increase statistics